J Mater Sci: Mater Med (2009) 20:2327–2336
DOI 10.1007/s10856-009-3791-4

RGD-modified acellular bovine pericardium as a bioprosthetic scaffold for tissue engineering

Xiaochao Dong · Xufeng Wei · Wei Yi · Chunhu Gu · Xiaojun Kang · Yang Liu · Qiang Li · Dinghua Yi

Received: 25 February 2009 / Accepted: 21 May 2009 / Published online: 9 June 2009

Abstract Acellular biological tissues, including bovine pericardia (BP), have been proposed as natural biomaterials for tissue engineering. However, small pore size, low porosity and lack of extra cellular matrix (ECM) after native cell extraction directly restrict the seed cell adhesion, migration and proliferation and which is a vital problem for ABP's application in the tissue engineered heart valve (TEHV). In the present study, we treated acellular BP with acetic acid, which increased the scaffold pore size and porosity and conjugated RGD polypeptides to ABP scaffolds. After 10 days of culture in vitro, the human mesenchymal stem cells (hMSCs) attached the best and proliferated the fastest on RGD-modified acellular scaffolds, and the cell has grown deep into the scaffold. In contrast, a low density of cells attached to the unmodified scaffolds, with few infiltrating into the acellular tissues. These findings support the potential use of modified acellular BP as a scaffold for tissue engineered heart valves.

1 Introduction

Heart valve disease is a significant cause of mortality worldwide. Prosthetic valve implantation is the most common treatment for valvular disease. However, both Mechanical prosthetic valve and bioprosthetic heart valve have shortcomings, such as embolism, wane, and an inability to grow, making them unsuitable for treating congenital heart defects. Consequently, many researchers are now exploring tissue engineering strategies to develop live heart valves.

Bovine pericardium is not only the sources of the most popular bioprostheses used in cardiac surgery, but also a prospective scaffold for TEHV after acellular treatment. Compared with synthesized material that used in tissue engineering scaffold, Acelluar bovine pericardium (ABP) has advantages of good mechanical property. And ABP is composed of native extracellular matrices (ECMs), including collagen, elastin, and various glycosaminoglycans (GAGs) [1], and has been used as a natural biomaterial scaffold for tissue-engineered heart valves (TEHVs) [2–7]. These ECM components can bind to and modulate various proteins, including growth factors and cytokines essential for cellular adhesion, migration, proliferation, and differentiation [8].

Although ABPs have native ECMs that make them potential natural scaffolds for tissue engineering, their average pore size ($\sim$25 μm) and interconnectivity/porosity ($\sim$60%) are lower than those of synthetic scaffolds (250 μm and 90%) and are unsuitable for cell growth [9, 10]. Furthermore it was previously supposed that ABP had natural ECM components that could mimic the entire growth environment and mediate the cell adhesion cascade. However, results have since shown that it is hard for cells to grow after scaffold attachment, and no significant improvement is obtained compared to synthetic scaffolds.

The RGD sequence, a cell adhesion recognition motif found in materials such as collagen, fibronectin (FN), and tenascin C [11–13], is the ligand for integrin-mediated cell adhesion and is vital for cell behavior and cell cycle signaling [14]. The RGD sequence is also the most effective

Xiaochao Dong and Xufeng Wei contributed equally to this work.

X. Dong · X. Wei · W. Yi · C. Gu · X. Kang · Y. Liu · Q. Li · D. Yi (✉)
Institute of Cardiovascular Surgery, Xijing Hospital, The Fourth Military Medical University, 17 Changle Western Road, Xi'an, Shaanxi Province 710032, People's Republic of China
e-mail: Yidh.fmmu@yahoo.com.cn; libidod@hotmail.com

cell recognition motif used to stimulate cell adhesion on artificial surfaces [15, 16]. Therefore, conjugating RGD polypeptides to a biomaterial scaffold should improve the efficiency of cell attachment and proliferation.

Heart valves form from cardiac cushions that protrude from the underlying myocardium, forming thin, tapered leaflets with a single endothelial cell layer and a central extracellular matrix (ECM) comprised of collagen, elastin, and glycosaminoglycans. Each component of the ECM is synthesized, enzymatically degraded, and maintained by a heterogenic resident population of interstitial cells dispersed throughout the leaflet. These valve interstitial cells (VICs) is made up of fibroblasts, smooth muscle cells, and myofibroblasts. Bone marrow-derived mesenchymal stem cells (MSCs) have some similar characteristics to native VICs, and are currently used as the prime candidates for TEHV [17]. MSCs have the potential to differentiate into a number of cell types and are easily accessible. Moreover they have good proliferative capacity and demonstrate immunological tolerance [18]. It has thus been concluded that MSCs may be a potential cell source for the tissue engineering of heart valves.

In this study, ABP was treated with AcOH after cell extraction, and RGD polypeptides were directly coupled to the scaffolds. We hypothesize that an RGD-modified, AcOH-treated porous ABP should support allogenic hMSCs adhesion, migration and proliferation. The cellular morphology and proliferation of the cell-seeded scaffolds were quantified with various biochemical assays.

2 Materials and methods

The study received ethical permission from the Fourth Military Medical University Ethical Committee, that gave consent for the use of bone marrow samples for research, that would otherwise be disposed of. The study complied with the Declaration of Helsinki.

2.1 Sample preparation

Unless otherwise noted, all reactions were performed at room temperature. Cellular components were removed from slaughterhouse BP using a modified previously reported method [5, 9]. The BP were incubated for 3 h in a hypotonic Tris buffer (TBS, pH 7.4) containing the protease inhibitor PMSF (0.35 mg/l), following which 1% Triton X-100 (Biosharp, USA) was added and incubated for 4 h at 4°C. Samples were thoroughly rinsed in Hank's balanced salt solution (HBSS), digested with DNase and RNase at 37°C for 1 h, extracted for 4 h with Triton X-100, then washed for 48 h in HBSS. Acellular tissues were immersed in AcOH (0.2 M) for 1 h, rinsed in phosphate-buffered saline (PBS) to neutralize the pH, and lyophilized.

2.2 Characterization of scaffolds

At least five samples from each group were fixed in 10% phosphate-buffered formalin for more than 4 h, paraffin-embedded, sectioned (5-μm thickness), and stained with hematoxylin and eosin (HE). Masson's trichrome, van Gieson, and safranin-O stains were used to visualize the collagen, elastic fibers, and GAGs, respectively [19–22]. The GAG content was measured using dimethylmethylene blue and heparin as a standard [23]. Pore sizes were quantified using light microscopy and ImagePro Plus (Media Cybernetics, USA), and porosities were determined by helium pycnometery [21].

Fresh BP, ABP and AcOH further treated ABP(AA) tissues are mechanically and optically anisotropic due to their preferential collagen fiber orientation [24, 25]. Dumbbell-shaped tissue strips were cut parallel to the preferential orientation [26]. Using an apparatus similar to one described previously [24], 5 samples from each group were mechanically tested at a constant speed of 10 mm/min on an Instron material testing machine (3342, USA) [26]. Mean sample thicknesses were obtained by micrometer (Digimatic Micrometer MDC-25P, Japan). Fracture was defined to occur at the first decrease in load during extension. Nominal stress was defined as the ratio of the load to the initial cross-sectional area ($A_{cs,i}$), fracture strain as the percent strain at fracture, ultimate tensile strength as the fracture force divided by $A_{cs,I}$, and fracture tension as the fracture load divided by the strip width. Denaturation temperatures were determined with a differential scanning calorimeter (Perkin-Elmer Model DSC 7, USA).

2.3 RGD preparation and conjugation

Some collagen-based scaffolds were covalently conjugated with RGD peptides, as described previously [27]. After hydrating AA tissues in PBS (pH 6.5) for 1 h, the aspartatic and glutamic acid carboxyl groups were reacted for 15 min with a PBS solution containing 1-ethyl-3-dimethylaminopropyl carbodiimide hydrochloride (0.5 mg/ml; EDC) and N-hydroxysuccinimide (0.7 mg/ml; NHS) (Pierce). Scaffolds were rinsed to remove excess EDC/NHS, reacted with the GRGDSP peptide (Sangon, Shanghai, 0.1 mg/ml) in PBS for 2 h, rinsed in distilled water, and air dried. To observe RGD conjugation, 3 samples in each test group were reacted with GRGDSP–Dansyl chloride (Sangon, 0.1 mg/ml) and observed by fluorescent microscopy (80I, Nikon, Japan). Samples directly reacted with GRGDSP–Dansyl chloride in PBS (pH 7.4) served as negative controls.

2.4 Cell culturing and scaffold seeding

2.4.1 hMSCs isolation and culture

The hMSCs were isolated from the bone marrow of healthy human donors aged 8–46 years. Briefly, a bone marrow suspension was loaded over an equal volume of Ficoll and centrifuged at 1800 rpm for 20 min. The top layer of mononuclear cells was collected, washed three times with DMEM, suspended in low glucose DMEM with 10% FCS, 100 μg/ml penicillin, 100 U/ml streptomycin, 4 mM L-alanyl-L-glutamine, and plated at a density of 2×10^5 cells/cm^2. At the third passage, the MSC isolates expressing CD105 (SH2), CD29, CD44, in the absence of CD45, MHC class II, CD31, CD14, CD34, B7, and vWF, were further analyzed. Cells were used between passages 3 and 7.

2.4.2 hMSCs seeding on scaffolds

Once they reached 50% confluency, the hMSCs were labeled for 48 h in vitro with 5-bromo-20-deoxyuridine (100 mg/ml; BrdU, Sigma, USA) [28]. The cells were then washed, harvested using a 0.05% trypsin solution, resuspended at 1×10^6 hMSCs in 10 ml of culture medium, and seeded onto unmodified and RGD-modified acellular tissues in a disk shape with a 10-mm diameter. Untreated cellular tissue served as a negative control. All samples were rinsed once in PBS and then in 0.1% peracetic acid (PAA) in HBSS for 15 min before cell seeding. Cells were adhered for 1 h, then unattached cells were removed with PBS. After 90 min of incubation, 20 ml of culture medium were added and incubated for 20 h.

2.4.3 Cellular attachment and proliferation

ABP, AA, RGD-modified ABP and AA (ABP-RGD, AA-RGD) tissues were seeded with cultured hMSCs. Three samples from each time-point were rinsed in Sorenson's buffer and fixed in 2% glutaraldehyde prior to SEM. Using standard preparation techniques, samples for SEM were dehydrated in graded alcohol (30–100%) followed by several exchanges in absolute alcohol, and chemically dried in hexamethyldisilizane. Samples were mounted on carbon stubs, coated with a 4-nm layer of gold (Hitachi E-1010 Ion Sputter, Japan), and photomicrographs used to determine the cell numbers were captured at 5 kV and 200–3000× with a low-voltage, high-resolution SEM (Hitachi S3400N, Japan). After 10 days of culture each sample stained with hematoxylin and eosin (H&E) to determine the ingrowth of cells.

DNA content was quantified with Hoechst Dye 33258 (Invitrogen, USA) to assess cell proliferation at 5 and 10 days. Briefly, cells were harvested from five samples of each group by incubating with 0.05% trypsin. Cells were centrifuged, lysed, and lysates were diluted 10 times and incubated in equal volume of 0.1 mg/ml Hoechest 33258 for 10 min in 96-well plates. Fluorescence was determined with a FLUOstar Optima fluorescent plate reader (BMG Labtech, Offenburg, Germany) at 350 nm excitation and 445 nm emission. A DNA standard curve was constructed to determine the DNA content in each sample.

To assess the metabolic activity, cell-seeded acellular, AcOH-treated, and RGD-modified tissues were each placed in a new 24-well plate, rinsed twice with HBSS, and incubated in 10% alamarBlue (Biosource) in HBSS at 37°C for 2 h. Cells incubated for the same length of time on similarly treated plates served as positive controls, while negative controls included ABP-only and alamarBlue-only groups. Fluorescence readings were captured at 528 nm (excitation) and 590 nm (emission) (FLx 800 Microplate Fluorescence Reader, Bio-Tek Instruments, USA). Standard curves were generated for proliferation rate calculations and correlations between the fluorescence and cell numbers. Interference by auto fluorescence of the ABP or media was not seen.

2.5 Statistical analysis

Statistical analysis was performed to determine differences between the measured properties of groups. One-way analysis of variance was performed and confidence intervals determined using a statistical program (SPSS, Version 12, USA). All data are presented as means with standard deviations.

3 Results

3.1 Ultrastructures of the samples

The BP displayed numerous intact cells embedded within the connective tissue matrix before cell extraction, while the acellular tissue had large pores with increased interconnectivity. The increased pore size could be attributed to protonization of the tissue amino groups (i.e., free amino groups on the collagen) via AcOH treatment, which can expel the adjacent structural collagen fibrils [9] (Fig. 1a–c). The average pore size, porosity, denaturation temperature, and ultimate tensile strength of the AcOH-treated acellular tissue were 162.2 ± 24.3 μm, 94.7 ± 1.8%, 73.9 ± 0.58°C, and 9.9 ± 0.8 MPa, respectively (Table 1).

Masson's trichrome revealed large open spaces (pores) within the AcOH-treated tissues, some of which were significantly larger than the others and non-spherical

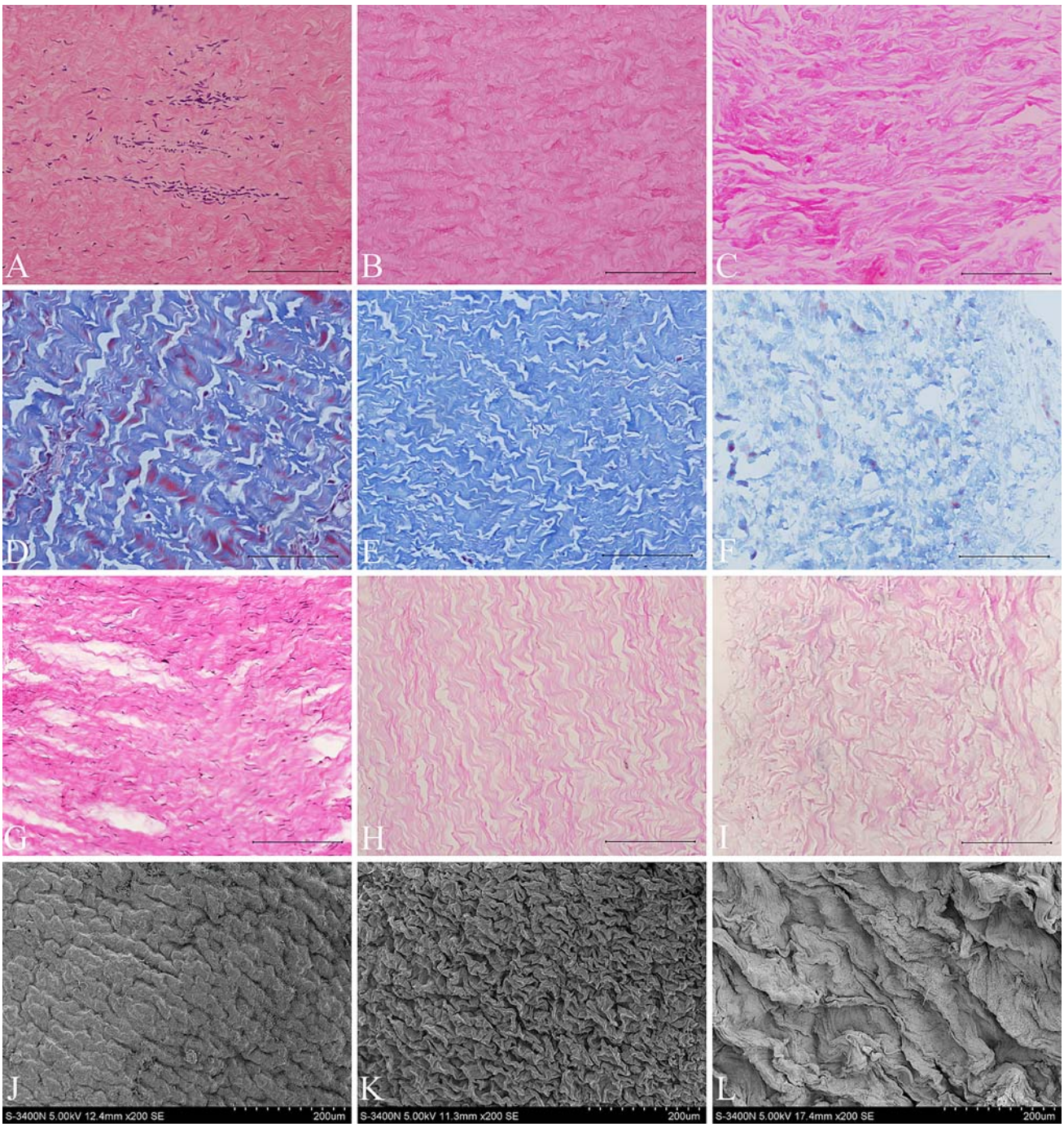

Fig. 1 HE staining (**a**–**c**), Masson's trichrome staining (**d**–**f**), Safranin-O staining (**g**–**i**) and SEM micrographs (**j**–**l**) of cellular (*left*), acellular (*middle*), and AcOH–treated acellular (*right*) tissues. Scale bars, 100 (**a**–**i**) μm

(Fig. 1d–f). The average distance between adjacent fibrils in the acellular tissue was significantly larger than that observed in the cellular tissue (Table 1). AcOH treatment increased the pore size significantly, with an average final size of ~160 μm in each direction. The porosities of the cellular (58.1%), acellular (67.3%), and AcOH-treated (94.7%) tissues also differed significantly (Table 1). SEM revealed no apparent differences in the surface morphologies of the cellular and acellular tissues. In contrast, collagen bundles on the AcOH-treated tissue surfaces were much looser (Fig. 1j–l).

3.2 Characterization of scaffolds

Safranin-O staining revealed comparable GAG contents of the acellular and AcOH-treated tissues, which were

Table 1 Measured physical, biophysical, and mechanical properties of each studied sample

Test samples[a]	Pore size (μm)	Porosity (%)	Denature temperature (°C)	Ultimate tensile strength (MPa)	GAG content (wt%)
Cellular tissue	N/A	58.1 ± 1.4%	76.7 ± 0.74	14.4 ± 1.1	0.68 ± 0.06
Acellular tissue	45.7 ± 10.5	67.3 ± 1.2%**	74.2 ± 0.44**	12.6 ± 0.6*	0.45 ± 0.08**
Acetic acid tissue	162.2 ± 24.3$^{\Delta\Delta}$	94.7 ± 1.8%**$^{\Delta\Delta}$	73.9 ± 0.58**	9.9 ± 0.8**$^{\Delta}$	0.43 ± 0.03**

[a] All results are given as the mean ± SD of $n = 5$ samples from each group. Compared with cellular tissue, * $P < 0.05$, ** $P < 0.01$; compared with acellular tissue, $^{\Delta}$ $P < 0.05$, $^{\Delta\Delta}$ $P < 0.01$

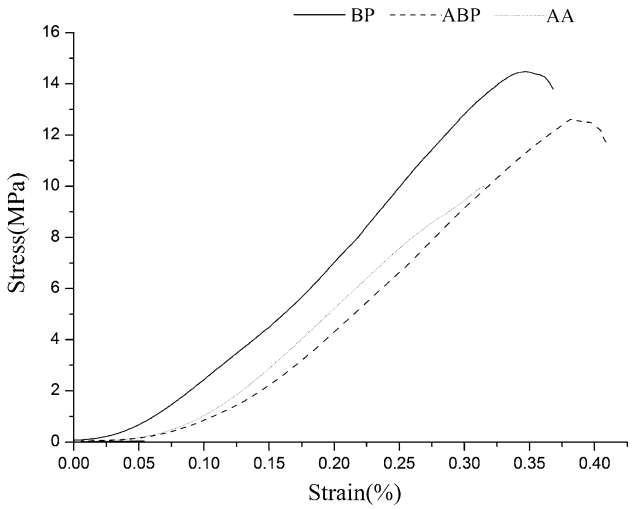

Fig. 2 Representative stress–strain curves for cellular, acellular and AcOH-treated acellular tissues

significantly lower than their cellular counterparts (Fig. 1g–i, Table 1). Compared with the cellular group, the denaturation temperatures of the acellular and AcOH-treated tissues were significantly reduced. No significant differences were found between the acellular and AcOH-treated groups (Table 1). The ultimate tensile strength of the acellular tissue decreased significantly after cell extraction (Fig. 2). That of the AcOH-treated tissue remained at 9.9 ± 0.8 MPa, though significantly lower than the cellular tissue group, it still remained good mechanical property compared with synthesized material, and suitable for tissue engineering applications (Table 1).

3.3 RGD-conjugated scaffolds and cell culture

The RGD peptide was effectively conjugated with the modified acellular scaffold, since GRGDSP–Dansyl chloride was highly positive in the AA and ABP groups, but the negative controls showed little fluorescence (Fig. 3). The hMSCs attached to the culture surface and showed a fibroblast-like appearance after 1 week in culture. Cells passaged once displayed a fibroblast-like, spindle-shaped morphology under phase contrast. Flow cytometry revealed the strong expression of CD44, CD166, and CD29, while CD34, CD45, CD14, and HLA-DR were not detected, confirming that the hMSCs were from a non-hematopoietic origin (data not shown). The immunophenotypic profile did not change after five passages, suggesting homogeneity.

3.4 Cell seeding on scaffolds

The hMSCs in the AA-RGD group proliferated faster than those in the ABP or AA groups at all five time points. After 10 days in culture and at the last four time points, significantly different cell numbers of hMSCs were found in the AA-RGD and ABP-RGD groups (Fig. 4a). Similar fluorescence readings were obtained for unseeded ABP- and alamarBlue-only controls, indicating that PAA successfully rendered any residual cells in the ABP nonviable. The DNA contents of the AA-RGD group at 5 and 10 days were 35.52 and 41.34 μg/scaffold, respectively, while those in the ABP-RGD group were significantly lower (29.73 and 31.97 μg/scaffold, respectively). The DNA contents of the ABP and AA groups were significantly lower than those of the AA-RGD group at 5 and 10 days (Fig. 4b).

SEM revealed that cells had attached to the ABP, AA, ABP-RGD, and AA-RGD tissues by 10 days of culture (Fig. 5). The AA-RGD sample clearly showed enhanced attachment; the cells appeared to have expanded, and the scaffold were embedded in a proliferating viable cell mass. Visually, cell attachment and expansion on the ABP were not as prolific as that on the RGD-modified ABP, and there was no significant cell expansion on the ABP scaffold. Significantly more hMSCs grew into the scaffold in the AA-RGD group, as indicated by HE staining; in the ABP group, only a single cell layer formed on the scaffold surface (Fig. 5).

Histological assessment revealed that the scaffold maintained its pore size, structure, and porosity after 10 days of culture in both groups. The AA-RGD group displayed a higher cell density than the other groups. The hMSCs grew predominantly along the micropores and displayed a semi-ovoid or spindle-shape morphology (Fig. 6).

4 Discussion

We treated ABP with AcOH, yielding scaffolds that displayed an increased pore size and porosity. Conjugation of

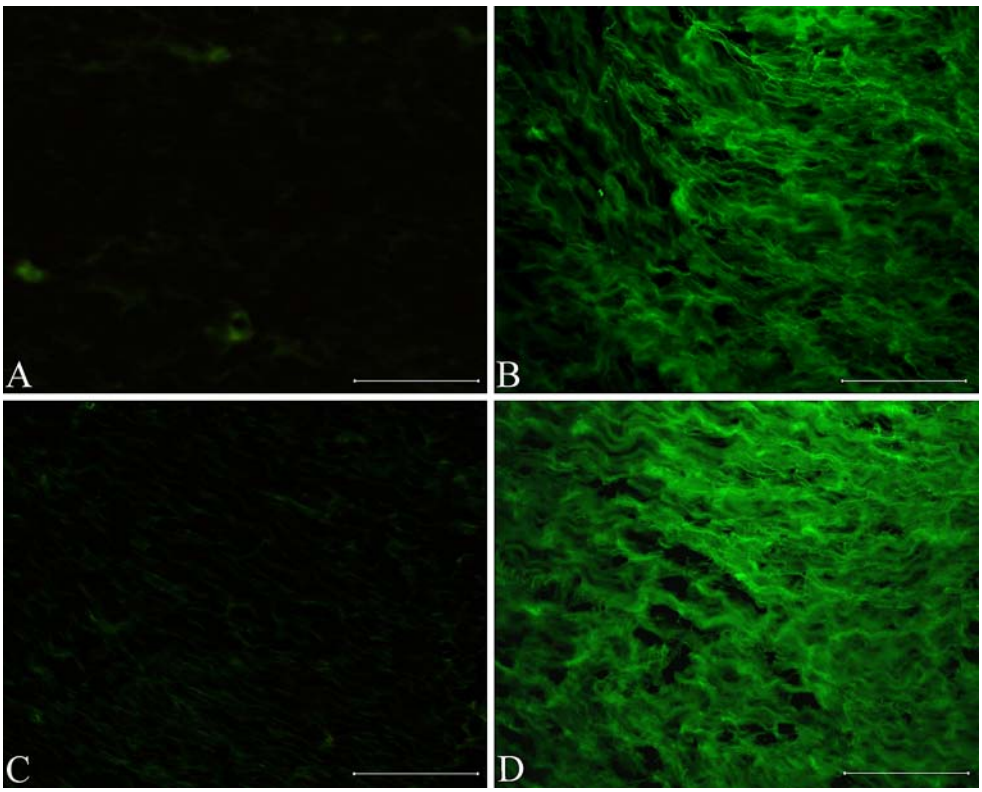

Fig. 3 RGD-Dansyl chloride conjugated on ABP (**a**, **b**) or AA (**c**, **d**) with only PBS (**a**, **c**) or with EDC/NHS (**b**, **d**). Scale bars, 100 μm

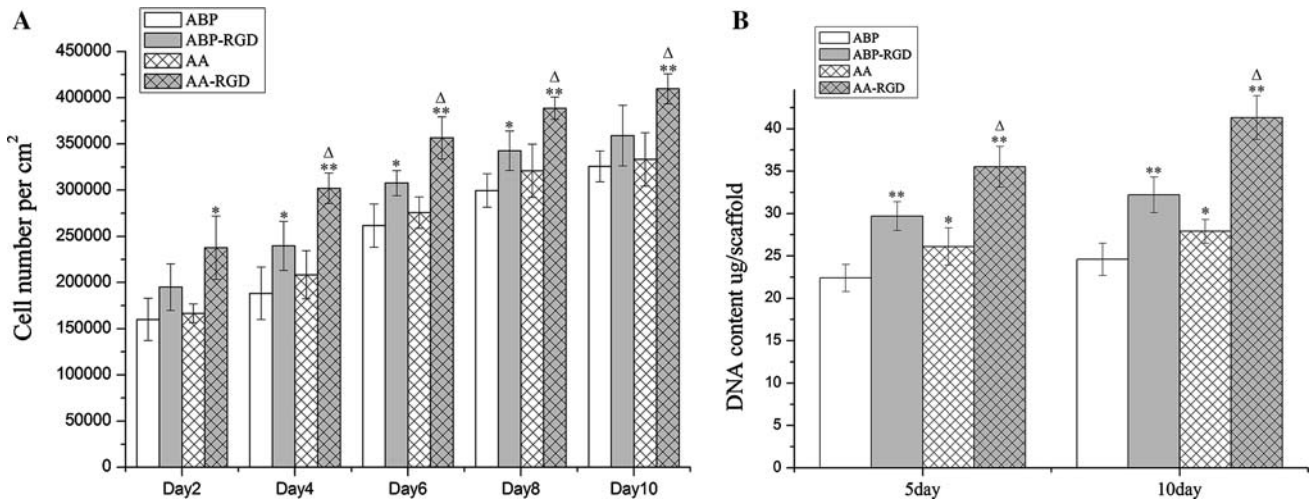

Fig. 4 **a** Cellular proliferation on BP, ABP, RGD-modified ABP and AA over 10 days as measured by alamarBlue. The MSCs number increases during the 10-d culture period. Compared with ABP, $^{*}P < 0.05$, $^{**}P < 0.01$; compared with ABP-RGD, $^{\Delta}P < 0.05$. **b** Quantification of DNA in the ABP, ABP-RGD, AA, AA-RGD groups at 5 and 10 days. Compared with ABP, $^{*}P < 0.05$, $^{**}P < 0.01$; compared with ABP-RGD, $^{\Delta}P < 0.05$

synthesized RGD polypeptides to these scaffolds further enhanced their cell adhesion ability. In contrast, a low density of cells attached to the unmodified scaffolds, with few infiltrating into the acellular tissues. Our findings support the further study of modified ABP as a potential scaffold for TEHVs.

A tissue-engineered ECM must be highly porous to be effective [29, 30], leading researchers to study methods to increase scaffold pore sizes. Although acellular biological scaffolds are more suitable than synthetic scaffolds for tissue engineering, we found that the pore size and porosity of ABP remained unsuitable for hMSC growth. To form

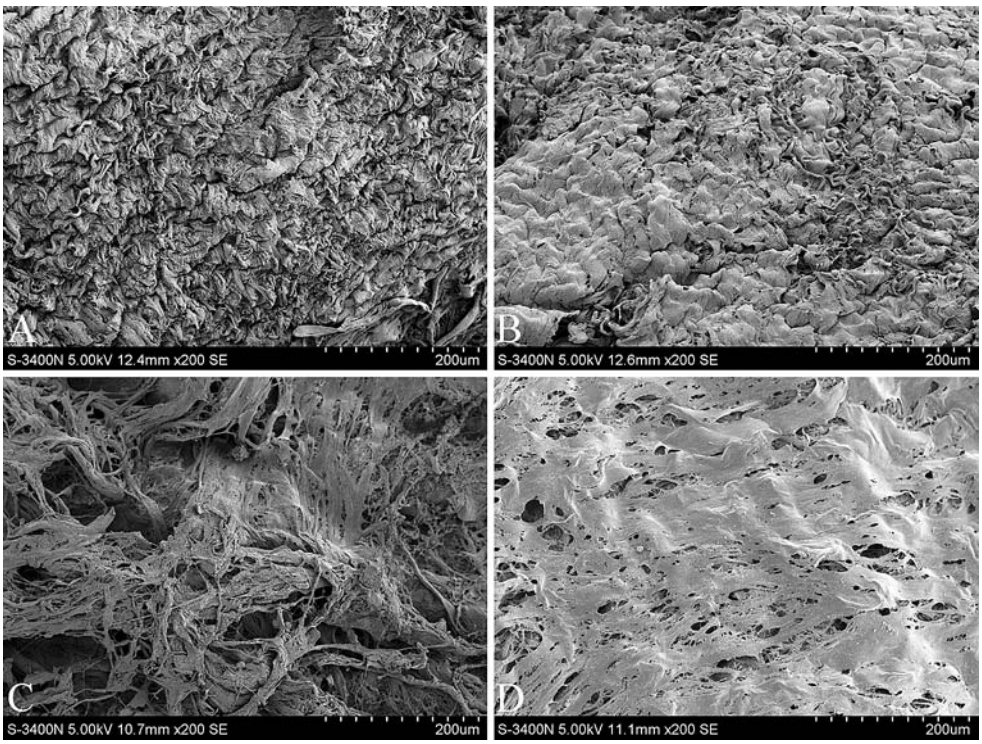

Fig. 5 Scanning electron photomicrographs depicting valvular cell proliferation on ABP (**a**), ABP-RGD (**b**), AA (**c**), AA-RGD (**d**) after 10 days in culture. The hMSCs form a confluent layer on the AA-RGD scaffold surface and long cytoplasmic extensions

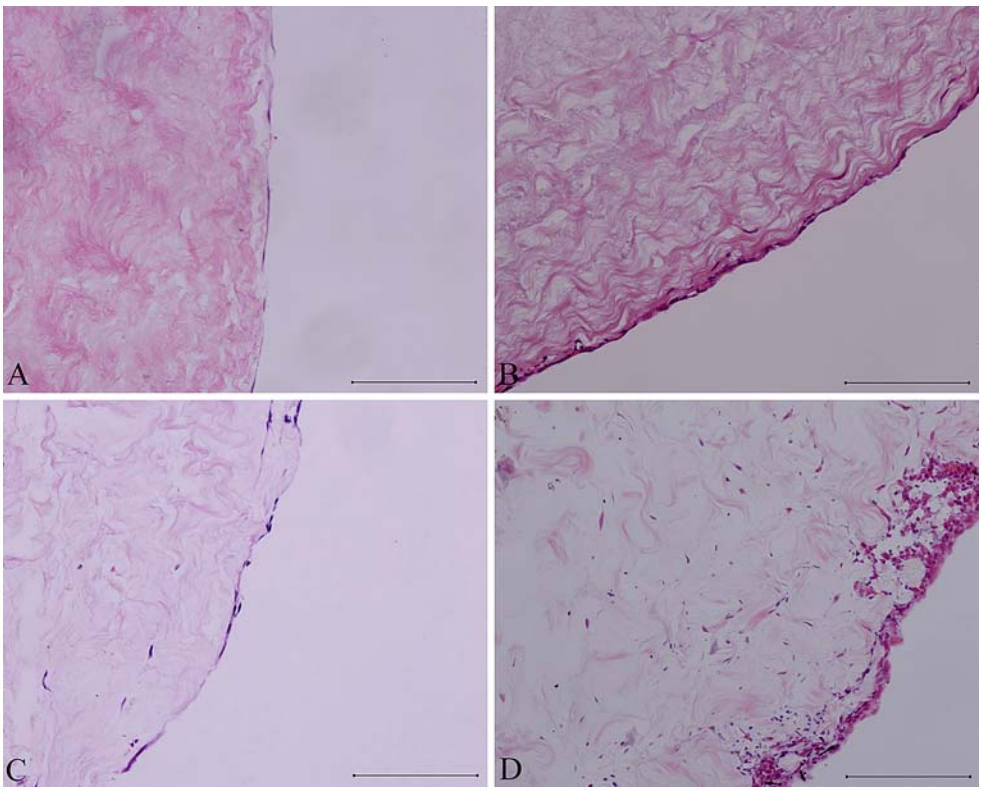

Fig. 6 HE stain after 10 days of culture on ABP (**a**), ABP-RGD (**b**), AA (**c**), and AA-RGD (**d**) in vitro. The MSCs grow deep into the scaffold in AA-RGD group, but form only a single layer on the surface of the scaffold in the AB group. Scale bars, 100 μm

distinct pore sizes and porosities within the matrix, we protonized the amino groups of the acellular tissues via AcOH treatment. This process substantially increased the distance between adjacent fibrils, significantly increasing the porosity and thickness of the AcOH-treated tissues compared to untreated acellular tissues (Table 1). Furthermore, tightly banded collagen fibers restrict nutrients and oxygen from the inner space of the BP. Acetic acid (AcOH) treatment can increase the pore size and porosity of these scaffolds, allowing increased in vitro seeded cell density, in vivo blood invasion, and oxygen and nutrient supply to the cells [31]. SEM revealed that the collagen bundles on the surface of the AcOH-treated tissue had become loose (Fig. 1).

The increased pore size and porosity associated with AcOH treatment may have been caused by increased water content, perhaps made possible by the removal of nonpolar lipids [5]. The AcOH-treated tissues showed substantial hMSCs infiltration into the scaffold interstices 10 days after cell seeding in vitro, compared to a low density of infiltrating hMSCs in the acellular tissues and nonexistent penetration into the cellular tissues (Fig. 6). Furthermore, the ultimate tensile strength was significantly reduced by cell extraction and AcOH treatment, which may be attributed to the greater pore size and porosity of these two groups. But still the value remained at nearly 10 MPa (Fig. 2), which was significantly higher than synthesized material [32].

RGD peptides were first identified by Pierschbacher and Ruoslahti as the minimal cell adhesion peptide sequence in FN [11]. Since then, RGD sequences have been identified in vitronectin, collagen, and membrane proteins [33]. All RGD sequences are recognized by at least one integrin, cell adhesion receptors that control various cell signaling pathways. Cells migrate on the ECM using integrins, and the covalent coupling of RGD peptides to a biomaterial surface increases cellular adhesion and growth [34, 35]. Thus, RGB peptides are often used to stimulate cell adhesion to synthetic surfaces [15, 36, 37].

We conjugated an RGD peptide to AcOH-treated ABP, to improve cell adhesion and growth. The RGD peptide could be tightly conjugated to the ABP scaffold by EDC/NHS (Fig. 3). Furthermore, hMSC adhesion on the acellular tissue was enhanced by the RGD peptide, due to the presence of collagen-linked RGD. Without RGD modification, the AcOH-treated acellular tissues displayed only a small improvement in scaffold cellularity over RGD-modified porous acellular tissues (Fig. 4a). Previous studies have also shown that cell attachment is dose-dependent on RGD modification levels.

Ten days after MSC implantation, the AA-RGD group showed significantly cell ingrowth in vitro. In contrast, the AcOH-treated ABP and RGD-modified acellular tissues had little ingrowth, and almost no cellular ingrowth occurred in the unmodified acellular tissue group (Fig. 6). The DNA contents at 5 and 10 days in the AB-RGD, AA, and AA-RGD groups were significantly higher than in the AB group, and were significantly different between the AA-RGD and AB-RGD groups (Fig. 4b). These results indicate that a proper pore size and porosity may improve cellular ingrowth, and that conjugated RGD peptides efficiently enhance cell adhesion.

The expression and organization of the ECM are critical for native tissue and engineered constructs. The ECM is a dynamic entity that signals or cues adherent cells to store or release bioactive factors, and thus controls many aspects of cellular behavior. After coupling RGD peptides, more hMSCs attached to the acellular tissues and expressed various integrins and ECM components, particularly those pertinent to valve integrity. Selective ECM expression by MSCs has previously been demonstrated at the RNA level [38]. Both MSCs and ICs express collagen I over time and deposit it extracellularly. This behavior is crucial in valve tissue engineering, as collagens comprise 60% of the total ECM content of the valves [39] and provide strength to the tissue.

5 Conclusions

Fresh BP cells were extracted and treated with AcOH to enlarge the inner space of the acellular tissue. After AcOH treatment, the tissue still remained good mechanical property. Furthermore, with RGD peptides modification the adhesion and proliferation of MSCs enhanced significantly. These findings support the hypothesis that modified with AcOH and RGD peptides ABP may serve as a potential scaffold for TEHVs. Future studies may involve the creation of the incorporation of additional biomolecules within the scaffold, and investigations into MSC differentiation.

Acknowledgements This work was supported by a grant from National Natural Science Foundation of China (No. 30672086, NO. 30600137) and National High-tech Research and Development Program (863 Program) of China (No. 2006AA02A138).

References

1. Lai PH, Chang Y, Chen SC, Wang CC, Liang HC, Chang WC, et al. Acellular biological tissues containing inherent glycosaminoglycans for loading basic fibroblast growth factor promote angiogenesis and tissue regeneration. Tissue Eng. 2006;12(9):2499–508. doi:10.1089/ten.2006.12.2499.
2. Schmidt CE, Baier JM. Acellular vascular tissues: natural biomaterials for tissue repair and tissue engineering. Biomaterials. 2000;21(22):2215–31. doi:10.1016/S0142-9612(00)00148-4.
3. Guldner NW, Jasmund I, Zimmermann H, Heinlein M, Girndt B, Meier V, et al. Detoxification and endothelialization of

glutaraldehyde-fixed bovine pericardium with titanium coating: a new technology for cardiovascular tissue engineering. Circulation. 2009;119(12):1653–60. doi:10.1161/CIRCULATIONAHA.108.823948.
4. Chang Y, Tsai CC, Liang HC, Sung HW. In vivo evaluation of cellular and acellular bovine pericardia fixed with a naturally occurring crosslinking agent (genipin). Biomaterials. 2002; 23(12):2447–57. doi:10.1016/S0142-9612(01)00379-9.
5. Courtman DW, Pereira CA, Kashef V, McComb D, Lee JM, Wilson GJ. Development of a pericardial acellular matrix biomaterial: biochemical and mechanical effects of cell extraction. J Biomed Mater Res. 1994;28(6):655–66. doi:10.1002/jbm.820280602.
6. Hodde J. Naturally occurring scaffolds for soft tissue repair and regeneration. Tissue Eng. 2002;8(2):295–308. doi:10.1089/107632702753725058.
7. Elizabeth DH. Cell biology of extracellular matrix. New York: Plenum Press; 1991.
8. Stringer SE, Gallagher JT. Heparan sulphate. Int J Biochem Cell Biol. 1997;29(5):709–14. doi:10.1016/S1357-2725(96)00170-7.
9. Wei HJ, Liang HC, Lee MH, Huang YC, Chang Y, Sung HW. Construction of varying porous structures in acellular bovine pericardia as a tissue-engineering extracellular matrix. Biomaterials. 2005;26(14):1905–13. doi:10.1016/j.biomaterials.2004.06.014.
10. Li J, Mak AFT. Transfer of collagen coating from porogen to scaffold: Collagen coating within poly(DL-lactic-co-glycolic acid) scaffold. Compos. B. 2007;38:317–23. doi:10.1016/j.compositesb.2006.06.009.
11. Pierschbacher MD, Ruoslahti E. Cell attachment activity of fibronectin can be duplicated by small synthetic fragments of the molecule. Nature. 1984;309:30–3. doi:10.1038/309030a0.
12. Cutler SM, Garcia AJ. Engineering cell adhesive surfaces that direct integrin alpha5beta1 binding using a recombinant fragment of fibronectin. Biomaterials. 2003;24(10):1759–70. doi:10.1016/S0142-9612(02)00570-7.
13. Jang JH, Hwang JH, Chung CP. Production of recombinant human tenascin-C module containing a cell adhesion recognition motif of RGD. Biotechnol Lett. 2004;26(24):1831–5. doi:10.1007/s10529-004-6031-5.
14. Chen CS, Alonso JL, Ostuni E, Whitesides GM, Ingber DE. Cell shape provides global control of focal adhesion assembly. Biochem Biophys Res Commun. 2003;307(2):355–61. doi:10.1016/S0006-291X(03)01165-3.
15. Hersel U, Dahmen C, Kessler H. RGD modified polymers: biomaterials for stimulated cell adhesion and beyond. Biomaterials. 2003;24(24):4385–415. doi:10.1016/S0142-9612(03)00343-0.
16. Rammelt S, Illert T, Bierbaum S, Scharnweber D, Zwipp H, Schneiders W. Coating of titanium implants with collagen, RGD peptide and chondroitin sulfate. Biomaterials. 2006;27(32):5561–71. doi:10.1016/j.biomaterials.2006.06.034.
17. Sutherland FW, Perry TE, Yu Y, Sherwood MC, Rabkin E, Masuda Y, et al. From stem cells to viable autologous semilunar heart valve. Circulation. 2005;111(21):2783–91. doi:10.1161/CIRCULATIONAHA.104.498378.
18. Aggarwal S, Pittenger MF. Human mesenchymal stem cells modulate allogeneic immune cell responses. Blood. 2005;105(4): 1815–22. doi:10.1182/blood-2004-04-1559.
19. Young B HJ. Wheater's functional histology. New York: Churchill Livingstone; 2000.
20. Sandberg LB, Soskel NT, Leslie JG. Elastin structure, biosynthesis, and relation to disease states. N Engl J Med. 1981; 304(10):566–79.
21. Martin I, Shastri VP, Padera RF, Yang J, Mackay AJ, Langer R, et al. Selective differentiation of mammalian bone marrow stromal cells cultured on three-dimensional polymer foams. J Biomed Mater Res. 2001;55(2):229–35. doi:10.1002/1097-4636(20010505)55:2<229::AID-JBM1009>3.0.CO;2-Q.
22. Wayne JS, McDowell CL, Willis MC. Long-term survival of regenerated cartilage on a large joint surface. J Rehabil Res Dev. 2001;38(2):191–200.
23. Farndale RW, Buttle DJ, Barrett AJ. Improved quantitation and discrimination of sulphated glycosaminoglycans by use of dimethylmethylene blue. Biochim Biophys Acta. 1986;883(2):173–7.
24. Lee JM, Haberer SA, Boughner DR. The bovine pericardial xenograft: I. Effect of fixation in aldehydes without constraint on the tensile viscoelastic properties of bovine pericardium. J Biomed Mater Res. 1989;23(5):457–75. doi:10.1002/jbm.820230502.
25. Simionescu D, Simionescu A, Deac R. Mapping of glutaraldehyde-treated bovine pericardium and tissue selection for bioprosthetic heart valves. J Biomed Mater Res. 1993;27(6):697–704. doi:10.1002/jbm.820270602.
26. Sung HW, Chang Y, Chiu CT, Chen CN, Liang HC. Crosslinking characteristics and mechanical properties of a bovine pericardium fixed with a naturally occurring crosslinking agent. J Biomed Mater Res. 1999;47(2):116–26. doi:10.1002/(SICI)1097-4636(199911)47:2<116::AID-JBM2>3.0.CO;2-J.
27. Chen J, Altman GH, Karageorgiou V, Horan R, Collette A, Volloch V, et al. Human bone marrow stromal cell and ligament fibroblast responses on RGD-modified silk fibers. J Biomed Mater Res A. 2003;67(2):559–70. doi:10.1002/jbm.a.10120.
28. Krupnick AS, Kreisel D, Engels FH, Szeto WY, Plappert T, Popma SH, et al. A novel small animal model of left ventricular tissue engineering. J Heart Lung Transplant. 2002;21(2):233–43. doi:10.1016/S1053-2498(01)00349-7.
29. Matsuda T, Nakayama Y. Surface microarchitectural design in biomedical applications: in vitro transmural endothelialization on microporous segmented polyurethane films fabricated using an excimer laser. J Biomed Mater Res. 1996;31(2):235–42. doi:10.1002/(SICI)1097-4636(199606)31:2<235::AID-JBM10>3.0.CO;2-K.
30. Nehrer S, Breinan HA, Ramappa A, Young G, Shortkroff S, Louie LK, et al. Matrix collagen type and pore size influence behaviour of seeded canine chondrocytes. Biomaterials. 1997; 18(11):769–76. doi:10.1016/S0142-9612(97)00001-X.
31. Kim BS, Baez CE, Atala A. Biomaterials for tissue engineering. World J Urol. 2000;18(1):2–9. doi:10.1007/s003450050002.
32. Mirani RD, Pratt J, Iyer P, Madihally SV. The stress relaxation characteristics of composite matrices etched to produce nanoscale surface features. Biomaterials. 2009;30(5):703–10. doi:10.1016/j.biomaterials.2008.10.023.
33. Ruoslahti E, Pierschbacher MD. New perspectives in cell adhesion: RGD and integrins. Science. 1987;238(4826):491–7. doi:10.1126/science.2821619.
34. Burdick JA, Anseth KS. Photoencapsulation of osteoblasts in injectable RGD-modified PEG hydrogels for bone tissue engineering. Biomaterials. 2002;23(22):4315–23. doi:10.1016/S0142-9612(02)00176-X.
35. Massia SP, Hubbell JA. Human endothelial cell interactions with surface-coupled adhesion peptides on a nonadhesive glass substrate and two polymeric biomaterials. J Biomed Mater Res. 1991;25(2):223–42. doi:10.1002/jbm.820250209.
36. Beuvelot J, Portet D, Lecollinet G, Moreau MF, Basle MF, Chappard D, et al. In vitro kinetic study of growth and mineralization of osteoblast-like cells (Saos-2) on titanium surface coated with a RGD functionalized bisphosphonate. J Biomed Mater Res B Appl Biomater. 2009.
37. Lin YC, Brayfield CA, Gerlach JC, Rubin JP, Marra KG. Peptide modification of polyethersulfone surfaces to improve adipose-derived stem cell adhesion. Acta Biomater. 2009;5(5):1416–24. doi:10.1016/j.actbio.2008.11.031.

38. Chichester CO, Fernandez M, Minguell JJ. Extracellular matrix gene expression by human bone marrow stroma and by marrow fibroblasts. Cell Adhes Commun. 1993;1(2):93–9. doi:10.3109/15419069309095685.

39. Bashey RI, Torii S, Angrist A. Age-related collagen and elastin content of human heart valves. J Gerontol. 1967;22(2):203–8.